ENGINEERING RESEARCH JOURNAL (ERJ)

Vol. 1, No. 39 Jan. 2019, pp. 23-31.

Journal Homepage: www.feng.bu.edu.eg

Enhancement Of the Surge Margin Of An Axial-Flow Fan Using Inlet Guide Vanes (IGV)

K. M. Almudahka[1] , Aly M. Elzahaby[2], Mohamed K. Khalil[3] , Ahmed F. Nemnem[4], Nader A. Elqussas[4]

[1] Master of Science Candidate – M.T.C.Egypt Royal Bahraini Air Force , [2] Prof.-Tanta University Mechanics Department M.T.C., Egypt , [3] Doctor, Head of Aircraft , [4] Doctor, Aircraft Doctor, Armed Forces Mechanics Department Egypt M.T.C., Egypt

Abstract. Improvement of the surge margin is carried out by the stall and surge control methods to allow a wider range of operation. This work shows the improved surge margin of an axial flow fan used as a power fan (which considered as a low-pressure-ratio compressor) in a wind tunnel by implementing an additional row of inlet guide vanes (IGVs) upstream of the rotor blades in order to redirect the entering flow to the suitable incidence angle for the rotor blades. Three different exit setting angles for IGVs row are tested by using a computational fluid dynamics (CFD) model via the commercial program ANSYS. The fan measured data sheet[1] and a baseline case are compared to validate the design point of the constructed CFD model.

The fan flow path, the mean line total conditions and all design controlling parameters are determined on the basis of mass, energy and momentum conservation equations. The solution presented is based on the finite volume technique, which is utilized by ANSYS CFX to solve those equations in order to calculate the flow characteristics.

The fan surge line is constructed first by the CFD model (that consists of various rotor operating pitch angles for the fan) and the results are compared to the baseline case and found with a deviation of about 3.644%. The IGVs with different setting angles are placed in **the** CFD model one at
a time for all rotor blade pitch angles upstream of the rotor blades and the new surge lines are achieved for each.

Finally, the selected control law for IGVs setting angle variation is introduced with an improved surge margin by about 12% and 37.931% for the pitch angles +5° and -15°, respectively.

Keywords : Axial flow fan, Surge margin, Inlet guide vanes (IGV), Wind Tunnel Fan, Power Fan.

1. INTRODUCTION

In order to achieve the desired compression ratio and flow characteristics, fans and compressors typically operate near the stall line, hence a satisfactory stall margin should be achieved and maintained at every condition[2].

Many stall and surge control methods were implemented over the years to stabilize the compressor in the critical range of operation, hence attain a wider range of operations. One of these control methods is the injection of air either upstream or downstream the rotor blade.

Behnken[3] stated that the idea of injecting air helps shifting the steady state of the compressor characteristics. The actuation of injectors were tested on Moore Greitzer compression system model. The closed loop feedbackand simulation can determine the optimal injector position inside the stall cell and can be utilized to reduce the hysteresis region of rotating stall.

Day[4] successfully experimented injection method with two approaches on a four-stage compressor in order to suppress the onset rotating stall and surge. First approach was to inject air via fast-acting valves by small amount (as low as 1% of the main mass flow rate) and found that the pre-stall perturbations were damped out leading to a 4% improvement in the surge margin. The second approach was to inject air in the vicinity of the stall cell. A 6% improvement of the surge margin was found.

Another method usually used is the recirculation method. Hathaway[5] used a CFD model to simulate and evaluate the effects of recirculation method on compressor performance. A compressor with self-recirculating casing treatment was simulated. As stall approaches, end wall blockage occurs due to low relative total pressure fluid. By implementing the recirculation method, the total pressure was

raised and the surge margin was extended without any efficiency loss.

Zhang[6] performed a numerical experiment on an end wall self-recirculating axial-flow compressor in order to evaluate its effects on the compressor performance. The numerical results proved that this method is capable of suspending the stall and improve the compressor efficiency at the same time.

Furthermore, inlet guide vanes (IGVs) are widely used by many researchers and engineers. Li and Lin[7] Used IGVs method due to its capability of achieving high efficiency and maintaining a stable operation of the compressor. They enhanced the compressor's efficiency by changing the stagger angle of the IGVs according to the flow characteristics. They proved that the rotor blade inlet angle of attack can be moderated by altering the stagger angle of the IGVs to obtain the optimum efficiency at a given condition. Moreover, the change of the coefficient of pressure rise is little when compared to the amount of enhancement of efficiency, thus the experiment is potential upon application.

Ling and Sönne[8] implemented different IGVs setting angles to achieve the optimum compressor performance and efficiency via controlling the intake area and air velocity. They proved that the more opened IGVs position, the higher the risk of surge, due to higher pressure-ratios in the front stages than the last stages. Hence an optimized IGVs setting angle is required.

Rajesh and Roy[9] stated that the presence of the IGVs plays an important part in keeping the compressor from stalling. The compressor performance can be enhanced by adjusting the IGVs setting angle to meet the rotor requirements. They concluded by stating that IGVs improve the operating range of the compressor.

Rukavina[10] stated that IGVs are a solution to delay the occurrence of the rotating stall in compressors. He tested two compressors, one with fixed IGVs and the other with adjustable IGVs setting angles. His test results showed an enhancement of both stall recovery and surge margin in low speed compressors if the IGVs setting angle is set right.

The previous studies showed the importance and benefits of using IGVs as a stall avoidance method, therefore their application is studied in this work to determine their effects on delaying the onset of rotating stall and enlarging the surge margin of an axial flow fan which leads to a wider range of operations.

Setting angle of the IGVs is a crucial parameter in achieving the highest performance of the fan as proven in the mentioned studies. However, large increments of the IGVs setting angles will deteriorate the efficiency and the pressure ratio downstream of the fan, thus the risk of surge will be coupled to the upstream of the fan[11],[7],[8] due to the blockage of the inlet area and the increasing air velocity. Herein, different IGVsexit setting angles are tested to differentiate their surge margins improvement for each case, which will be discussed furthermore.

2. GEOMETRY AND MODELING

2.1 Fan Geometry

The fan selected for this work is wind tunnel power fan WAF22-4-10[1] which operates at a constant speed n=740 rpm, with 10 rotor blades of an outer diameter of 2.240m and an inner diameter of 1m. The blade length is 0.62m and the rotor blade pitch angle (β) can be altered hydraulically as desired from 5°, 0°, -5°, -10° and -15° in order to obtain the fan characteristic curves.

The fan blades geometry at different pitch angles are taken from M. Khalil[1]. By using the previous data, a 3D blade model is constructed, as shown in Fig. (1), via ANSYS BladeGen for each case.

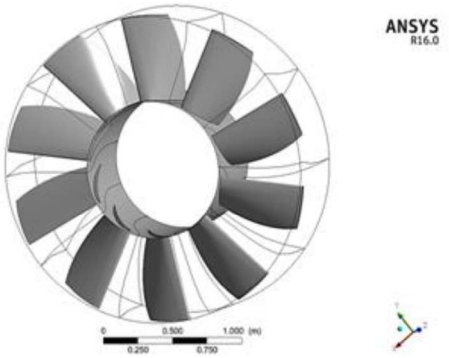

Fig. (1) Isometric View of the Fan Blade Row Generated by ANSYS BladeGen

2.2 Inlet Guide Vanes (IGVs) Geometry

The 3D IGVs are based on NACA-65 airfoil because it permits wide-ranging of laminar flow which can simplify the turbulence and hysteresis occurred within a stall/surge and it has a satisfactory critical speed characteristics than other airfoils[12]. Thereafter, the IGV profile is constructed by a MATLAB code. Three different IGVsexit setting angles are chosen 0°, 3° and 5° in order to distinguish the difference in the stall margins they will produce when put upstream of the rotor blades, hence selecting the best setting angle for the desired application and given data. The IGVs are with no twist in order to keep the entering flow as laminar as possible

and to eliminate the whirl effect caused by the radial rotation of the IGVs when applied.

The formula needed to calculate the number of IGVs (Z) can be derived from the blade solidity ratio as follows:

$$\text{Blade solidity} = \frac{c}{s} \quad (1)$$

Where

c … length of the blade chord line

s … pitch or staggered (blade) spacing

$$\text{Since, } s = \frac{\pi . D_m}{Z} \quad (2)$$

$$\text{Hence, } \frac{c}{s} = \frac{c.Z}{\pi . D_m} \quad (3)$$

Therefore, the number of blades is the circumference of the mean line divided by the blade (staggered) spacing, as follows:

$$Z = \frac{\pi \, . \, D_m}{s} \quad (4)$$

Where:

Z … the number of IGVs

D_m … mean diameter

The mean diameter can be determined by solving the following formula:

$$D_m = \frac{D_O + D_I}{2} \quad (5)$$

Where

D_O … the outer diameter

D_I … the inner diameter

Since the optimum pitch to chord ratio $(s/c)_{opt}$ ranges between 0.75 and 0.85[13]. It has been decided after few trials that $(s/c)_{opt}$ should be 0.85, and as shown in Fig. (2), the IGVs chord c= 40 cm, hence:

s = c * 0.85 = 40 * 0.85 = 34 cm

From equation (5), $D_m = \frac{1+2,24}{2}$ = 1.62m

Thus, $Z = \frac{3.14*162}{34}$ = 14.9688 ≈ 15

The different setting angles of the IGVs are reached by tilting the rear half of the IGV blade to the required angle, as shown in Fig. (2).

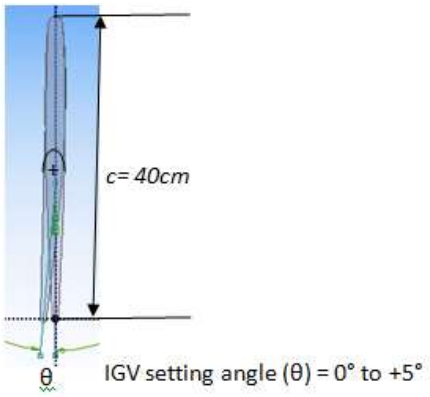

Fig. (2) IGV Chord and (θ)

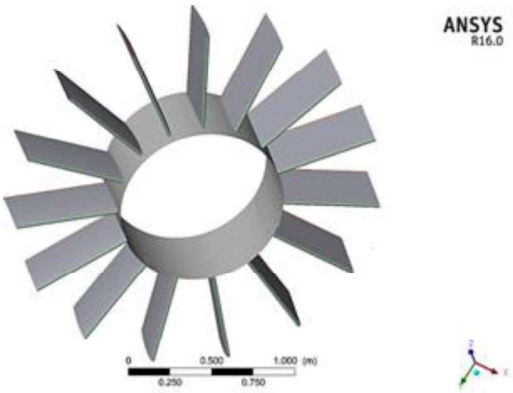

Fig. (3) Isometric View of the IGV Row at 0° Setting Angle

Different surge margin improvements of the fan are tested by implementing each IGV setting angle (θ) with each pitch angle of the rotor (β).

2.3 Governing Equations

Any flow behavior can be defined and predicted by solving several partial differential equations that describe the processes of momentum, heat and mass transfer etc. These equations are known as the Navier-Stokes equations. ANSYS CFX is a solver engine that solves the unsteady Navier-Stokes equations in their conservation form in order to calculate the flow characteristics. The basic equations are:

a) The continuity equation:

$$(\partial\rho/\partial t) + \nabla . (\rho . \boldsymbol{U}) = 0 \quad (6)$$

Where

ρ… fluid density

t … time

U… the flow velocity vector field.

b) The momentum equation:

$$[\partial(\rho . \boldsymbol{U})/\partial t] + \nabla . (\rho . \boldsymbol{U} \times \boldsymbol{U}) = -\nabla p + \nabla \tau + \boldsymbol{S}_M \quad (7)$$

Where:

τ … the stress tensor.

c) The total energy equation:$[\partial(\rho htot)/\partial t]-(\partial p/\partial t)+\nabla.(\rho \boldsymbol{U} h_{tot})=\nabla .(\lambda \nabla T)+\nabla.(\boldsymbol{U}.\tau)+\boldsymbol{U}.\boldsymbol{S}_M$(8)

Where:

- the term $\nabla.(\boldsymbol{U}.\tau)$ expresses the work due to viscous stresses and called the viscous work term.

- the term $(\boldsymbol{U}.\boldsymbol{S}_M)$ expresses the work due to external momentum sources and is currently neglected.

d) The ideal gas Equation of State:

$$\rho = \frac{w.p_{abs}}{R_0.T} \quad (9)$$

Where:

w … molecular weight.

p_{abs} … the absolute pressure.

R_0 … the universal gas constant.

e)The Turbulence Model:

The two equations turbulence model$k$-ε based on Reynolds Averaged Navier-Stokes (RANS) equations is selected for this work.When executed with the flow equations will give the capability to simulate the flow behavior of real fluid. The main purpose of utilizing a turbulence model is to find a relationship between the unknown Reynolds stresses of turbulence and the known flow properties.

The commonly used simplified model for $k$is:

$$\frac{\partial(\rho k)}{\partial t} + div(\rho k U) = div\left[\frac{\mu_t}{\sigma_k} grad\, k\right] + 2\mu_t E_{ij}.E_{ij} - \rho\varepsilon \quad (10)$$

I II III IV V

Where:

I … rate of increase.

II … convective transport.

III … diffusive transport.

IV … rate of production.

V … rate of destruction.

σ_k… Prandtl number that connects the diffusivity of k to the eddy viscosity with a typical value of 1.

While the commonly used simplified model for $\varepsilon$is:

$$\frac{\partial(\rho\varepsilon)}{\partial t} + div(\rho\varepsilon U) = div\left[\frac{\mu_t}{\sigma_\varepsilon} grad\, \varepsilon\right] + C_{1\varepsilon}\frac{\varepsilon}{k}\mu_t E_{ij}.E_{ij} - C_{2\varepsilon}\rho\frac{\varepsilon^2}{k} \quad (11)$$

I II III IV V

Where:

I … rate of increase.

II … convective transport.

III … diffusive transport.

IV … rate of production.

V … rate of destruction.

σ_ε... Prandtl number that connects the diffusivity of ε to the eddy viscosity with a typical value of 1.3

$C_{1\varepsilon}$ … model constant with typical value of 1.44

$C_{2\varepsilon}$ … model constant with a typical value of 1.92

3.CFD SIMULATIONS

A detailed CFD model is created and performance simulations are executed to construct the fan characteristic map with and without the IGVs by evaluating the design parameters.

The computational domains, boundary conditions, meshing of the model and the solver control parameters are clarified in this section. The total head rise and the efficiency are compared to the baseline case results.

Flow simulation conditions of the fan domain are kept constant at a constant rpm. The simulation is repeated-by a certain number of iterations until convergence is achieved with fixed inlet total conditions and different mass flow rate values at the outlet where the domain total-to-total pressure and efficiency are calculated.

3.1 Model Meshing

TurboGrid is a subprogram within the ANSYS used to perform the process of fragmentation of the computational model into small cells. The included option of the Automatic Topology optimized (ATM optimized) is utilized in order to create a structured hexahedral cell that tracks the surface of the blade and is aligned with the flow direction. The number of elements in the mesh and the mesh size are also set.

Mesh independence test is carried out to guarantee that the results are independent to the mesh density and the two main calculated parameters are obtained for different mesh sizes, as shown in Table(1). Since the outcomes of the test were close to each other and the CFD model results should be in an acceptable range to the baseline case results, the mesh size of 1.4M nodes is selected due to the closeness of its results to the two key parameters, the total head rise and the efficiency, and to cut down the solution processing time.

Table (1) Mesh Independency Test

Number of nodes	Total Head Rise [pa]	Deviation [%]	Efficiency [%]	Deviation [%]
200K	1683	-	77	-
600K	1348.04	19.903	92	-19.481
800K	1878	-39.313	90.4	1.739
1.3M	1388	26.092	92.7	-2.544
1.4M	1399	-0.793	93	-0.324
3.5M	1361	2.716	93.2	-0.215

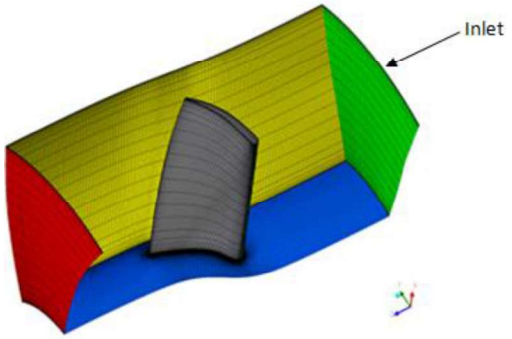

Fig. (4) Meshing of the Rotating Domain

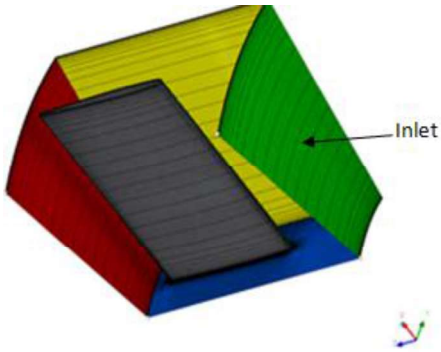

Fig. (5) Meshing of the IGV Domain

Figures (4) and (5) shows the structured mesh generated by TurboGrid with a clear view of their structure for the rotor and IGV domains, respectively.

3.2 Simulation Domains

The simulation of the axial fan domain is condensed in the passage of one IGV and one rotor blade cascade in order to decrease the calculations time and data size. This passage works as a sub-domain of the main domain of the fan which can be achieved by repeating this cascade in circumferential direction using symmetric feature.

The rotor domain rotates at a constant rotational speed n=740 rpm while the IGVs domain rests motionless. Due to the constant speed of the model, the constant flow direction, the solution convergent at automatic time-step and the flow is not supersonic, the steady-state analysis type is selected. Fig.(6) shows the cascade of the fan model including IGVs and rotor blades.

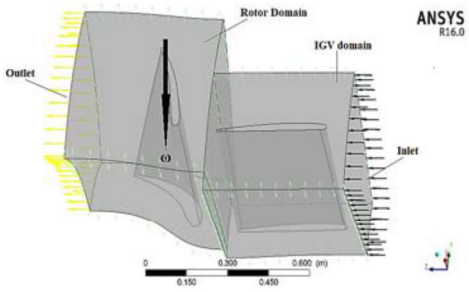

Fig. (6) IGV and Rotor Domains Cascade

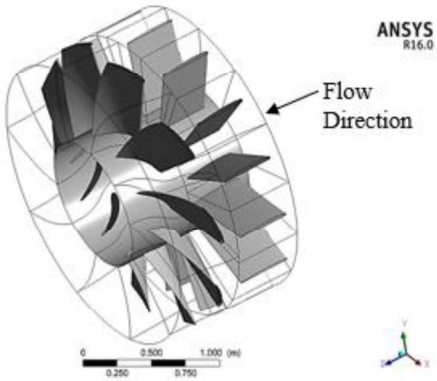

Fig. (7) Isometric View of the Simulated Domain

3.3 Boundary Conditions

The rotor blade, IGVs, shroud and hub surfaces are chosen as no-slip walls. The interface between IGVs and rotor domains is selected as total pressure conservation, known as the frozen rotor interface, because the appropriate frame transformation and pitch changes are made and accounted for, Fig.(8).

The inlet boundary conditions are set as total pressure and total temperature, while the outlet boundary condition is chosen as a mass flow rate values that change along the operating line with each simulation to construct the operating line using CFX results. In addition, obtaining the stall onset point for each case by monitoring the velocity vector field and the total pressure rise slope, Fig. (10).

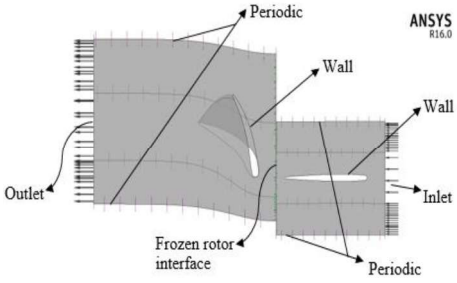

Fig. (8) Boundary Conditions Definitions in blade-to-blade Plane

Table (2) Boundary Conditions for the Simulation Domains

Feature	Boundary condition	Comment
Inlet	Total pressure and total temperature	Stationery
Outlet	Mass Flow Rate	Rotating
IGV hub	No slip wall	Stationery
Rotor hub	No slip wall	Rotating
IGV Shroud	No slip wall	Stationery
Rotor shroud	No slip wall	Rotating
Interface	Frozen rotor	Constant total pressure
IGV wall	No slip wall	Stationery
Rotor blade wall	No slip wall	Rotating

As known and suggested in turbomachinery simulations, the flow inside the passage is best to be modelled as three dimensional, steady, turbulent, compressible and viscous with a k-ε turbulence model, which has been selected for this work. The domain working fluid is set to be Ideal gas with the boundary conditions shown in Table (2).

3.4 CFD Model Performance Map

The performance map of the fan model is created by calculating different points on the performance curve via ANSYS CFX. The program runs a simulation with a constant 740rpm for all specified rotor pitch angles and IGVsexit setting angles at certain total pressure and total temperature at the inlet and a selected mass flow rate at the outlet. This step is repeated at different mass flow rates in order to obtain different points on the performance curve and to finally locate the stall point for each case.

4. RESULTS AND DISCUSSION

4.1 Model Validation

According to the data provided by the fan manufacturer and included in the baseline case, the design point on which the fan was constructed is at 0° rotor pitch angle, 85 kg/s mass flow, 101318 Pa inlet total pressure and 288 K total temperature. These data are used as basic inputs in ANSYS CFX first simulations in order to achieve the basic fan model characteristic curves.

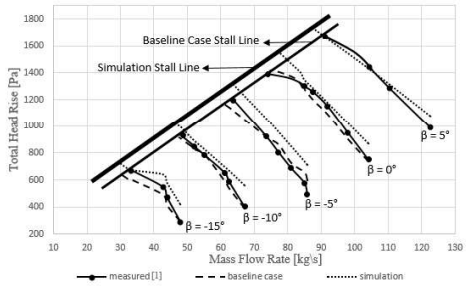

Fig. (9) Simulation Results Compared to the Measured and Baseline Case Results with Both Stall Lines Illustrated

The simulation outcomes of the basic fan model show a good agreement to the measured data in terms of the characteristic map operation lines. However, it is noticed that the CFD model results of total head rise are higher than those of the measured characteristics, as shown in Fig. (9). These small differences can be referred to the lack of both human and instruments error involved in the execution of experiments.

4.2 Simulation Results

In order to detect the stall onset point, the blade-to-blade velocity field vectors and total pressure rise slope are used. Fig. (10) shows the beginning of stall for a rotor blade mid-section at 0° pitch angle without IGV where the velocity drops and the flow starts to separate from the blade at the last quarter near the trailing edge.

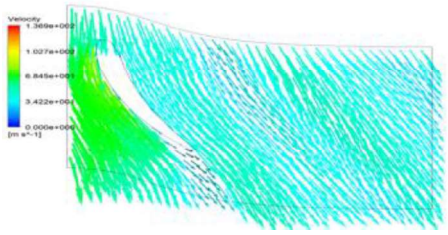

Fig. (10) The Beginning of Stall at Mean Section of 0° Pitch Angle Rotor Blade without IGVs

Once IGVs are implemented, the velocity distribution of the rotor blade at the same mass flow rate is uniformed and the flow behaves normally without signs of flow separation or stall onset as shown in Fig. (11) for all IGV setting angles. The velocity on the suction side of the rotor blade near the trailing edge increases by increasing the IGVs exit setting angle which enhance the boundary layer and prevent flow separation.

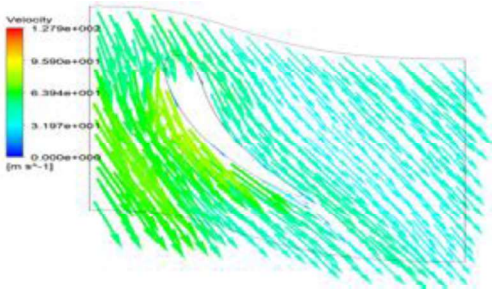

(a) Rotor Blade Mean Section with 0° IGVs

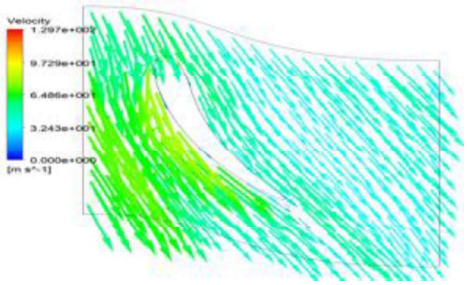

(b) Rotor Blade Mean Section with 5° IGVs

Fig. (11) 0° Pitch Angle Rotor Blade Mean Section with Different IGVs Setting Angles

Moreover, Fig. (12) shows that the stall point of the rotor blade shifts further to the left creating a larger surge margins at higher IGV setting angles. However, total head rise slightly decreases by increasing the IGV setting angle due to the accompanied friction losses. It is also noticed that the total head rise values have small differences when compared among the three IGV setting angles results. The isentropic efficiency of the fan stage shares the same qualities with the total head rise as seen in Fig. (13).

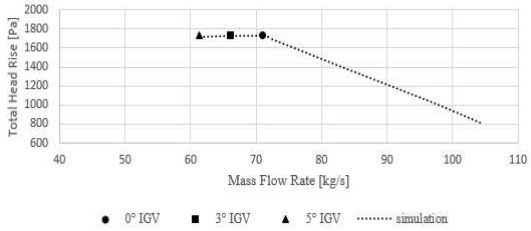

Fig. (12) Total Head Rise Versus Mass Flow Rate at 0° Pitch Angle Rotor Blade with all IGV Setting Angles Stall Points

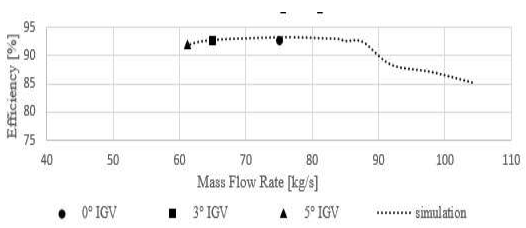

Fig. (13) Efficiency Versus Mass Flow Rate at 0° Pitch Angle Rotor Blade with all IGV Setting Angles Stall Points

Another example of a stall point with the flow separation is shown in Fig. (14) for the rotor blade at -15° pitch angle considering velocity vectors of blade-to-blade view at mean section. Without the IGVs, the same pattern of flow behaviour and velocity drop is found at mid-section rotor blade near the trailing edge. The IGV row has the same effect of maintaining the velocity in the normal operating range and correcting the incidence angle for the rotor blade at the same mass flow rate, hence the flow does not detach away from the blade before the trailing edge as shown in Fig. (15) for different IGV setting angles.

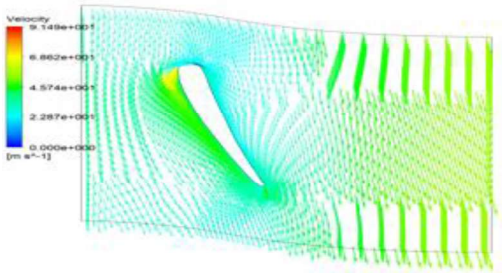

Fig. (14) The Beginning of Stall at Mean Section of -15° Pitch Angle Rotor Blade without IGVs

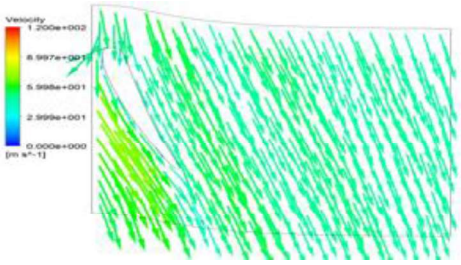

(a) Rotor Blade Mean Section with 0° IGVs

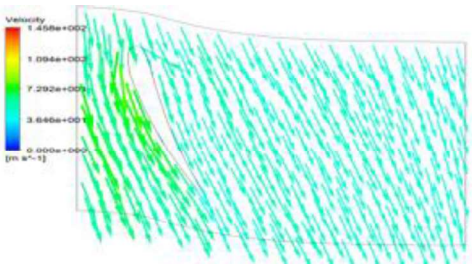

(b) Rotor Blade Mean Section with 5° IGVs

Fig. (15) -15° Pitch Angle Rotor Blade Mean Section with Different IGVs Setting Angles

The velocity at the suction side of the rotor blade trailing edge is increased by increasing the IGV setting angle as clearly shown in Fig.(15) which leads to an enhanced velocity distribution over the blade and a better pressure distribution as a result, thus a larger surge margin.

At the stall point of the rotor with 0° IGV setting angle, the total head rise is higher than that of the rotor stall point without IGV, as shown in Fig. (16). this is believed to be caused by the velocity rise of the rotor blade in the presence of the IGV row. Then, the total head rise will decrease by increasing the IGV setting angle like the previous case.

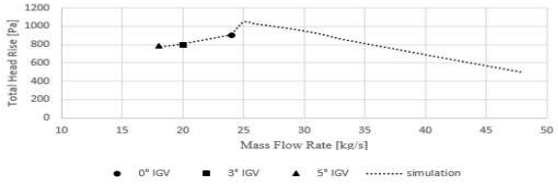

Fig. (16) Total Head Rise Versus Mass Flow Rate at -15° Pitch Angle Rotor Blade with all IGV Setting Angles Stall Points

As expected, the efficiency deteriorates by increasing the IGV setting angle as seen in Fig. (17). There is a significant drop of efficiency for the rotor with 3° IGV setting angle due to the drop of pressure and total head rise of this case.

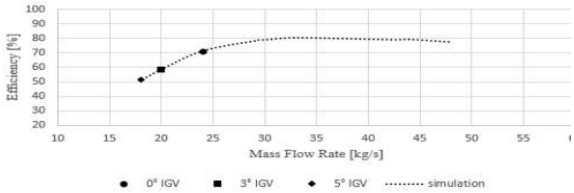

Fig. (17) Efficiency Versus Mass Flow Rate at -15° Pitch Angle Rotor Blade with all IGV Setting Angles Stall Points

As clearly shown in Fig. (18), the stall mass flow rate for each case gets lower with higher total pressure values, hence the surge lines are shifted further to the left with the increase of the IGV setting angle. This leads to a larger surge margin for each case. Unfortunately, both total head rise and isentropic efficiency of the fan stage are dropped with the increase of the IGV setting angle due to blockage and high velocities at the rotor blade inlet. Therefore, the selection of the IGV setting angle in the wind tunnel is potential to the desired tested model design parameters and operational characteristics.

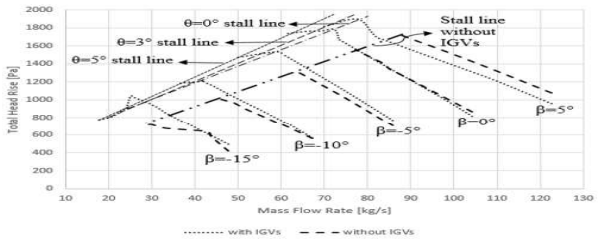

Fig. (18) Stall Lines for All Simulation Cases on the Model Characteristic Curves Map

According to the obtained results, the control law of IGVs setting angles (θ) variation is selected for all rotor pitch angles (β)as given in Table (3):

Table (3) (θ) Selection to (β) and the Surge Margin enhancement

θ [°]	0	2	3	4	5
β [°]	5	0	-5	-10	-15
S.M. Enhancement [%]	12	9.091	11.811	18.75	37.931

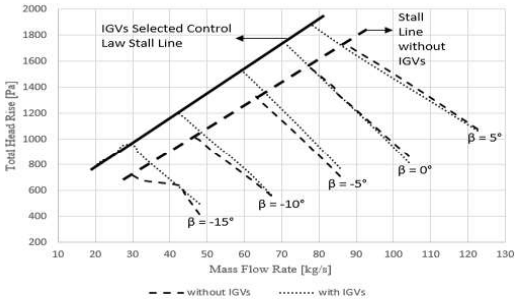

Fig. (19) Stall Line of IGVs Control Law versus Stall Line without IGVs in Characteristics Map

CONCLUSIONS

In this paper, inlet guide vanes (IGVs) are used as a stall control method in order to enhance the performance of a wind tunnel power fan by enlarging its surge margin. The IGV row is implemented upstream the fan row to redirect the entering flow to the suitable incidence angle of the rotor blades with 0°, 3° and 5° setting angles. The pitch angle of the fan blades can be altered hydraulically between 5°, 0°, -5°, -10° and -15°in order to obtain the fan characteristic curves. A full CFD model is constructed via the commercial program ANSYS. It consists of the fan blade row domain and the IGV row domain.

The IGVs with different setting angles are placed in the CFD model one at a time for all rotor blade pitch angles upstream of the rotor blades and the new surge lines are achieved for each one of them. After performing full CFD simulations on the fan model at all rotor pitch angles and IGV setting angles, new stall points are calculated by ANSYS CFX, hence all cases stall lines are drawn. The simulation results show an enhancement of the fan performance with the presence of the IGVs.

Finally, the selected control law for IGVs setting angle variation is introduced with an improved surge margin by about 12% to 37.9% for the pitch angles 5° to -15°, respectively.

REFERENCES

[1] M. K. K. Khalil, "Automation of Wind Tunnel Operation," Master of Science, Aircraft Mechanics-Mechanical Engineering, Military Technical College-Cairo, Military Technical College-Cairo, 2003.

[2] M. C. Huppert, "Some stall and surge phenomena in axial-flow compressors," *Journal of the Aeronautical Sciences,* vol. 20, pp. 835-845, 1953.

[3] R. L. Behnken, R. D'Andrea, and R. M. Murray, "Control of rotating stall in a low-speed axial flow compressor using pulsed air injection: Modeling, simulations, and experimental validation," in *Decision and Control, 1995., Proceedings of the 34th IEEE Conference on*, 1995, pp. 3056-3061.

[4] I. Day, "Active suppression of rotating stall and surge in axial compressors," *Journal of Turbomachinery,* vol. 115, pp. 40-47, 1993.

[5] M. D. Hathaway, "Self-recirculating casing treatment concept for enhanced compressor performance," in *ASME Turbo Expo 2002: Power for Land, Sea, and Air*, 2002, pp. 411-420.

[6] H.-g. ZHANG, W.-l. CHU, Y.-h. WU, P. GAO, and Y.-j. CAO, "Numerical investigation of the flow mechanisms of compressor stall delay through end wall self recirculation [J]," *Journal of Propulsion Technology,* vol. 2, p. 015, 2009.

[7] J. Li, F. Lin, C. Nie, and J. Chen, "Automatic efficiency optimization of an axial compressor with adjustable inlet guide vanes," *Journal of Thermal Science,* vol. 21, pp. 120-126, 2012
.

[8] S. Ling and T. Sönne, "VGV optimization for performance," 2014.

[9] E. Rajesh and B. Roy, "Numerical study of variable camber inlet guide vane on low speed axial compressor," in *ASME 2015 Gas Turbine India Conference*, 2015, pp. V001T01A022-V001T01A022.

[10] J. P. Rukavina and T. H. Okiishi, "Modification of axial-flow compressor stall margin by variation of stationary blade setting angles," IOWA STATE UNIV AMES DEPT OF MECHANICAL ENGINEERING1991.

[11] Y. Liu, Z. Lin, P. Lin, Y. Jin, T. Setoguchi, and H. D. Kim, "Effect of inlet guide vanes on the performance of small axial flow fan," *Journal of Thermal Science,* vol. 26, pp. 504-513, 2017.

[12] I. H. Abbott, A. E. Von Doenhoff, and L. Stivers Jr, "Summary of airfoil data," 1945.

[13] A. M. Elzahaby, "Theory of Jet Engines, Printed Lectures," M.T.C., Ed., ed, 1988.